Ultrafast Spin-State Dynamics in Transition-Metal Complexes Triggered by Soft-X-Ray Light

Huihui Wang,[1] Sergey I. Bokarev,[1,*] Saadullah G. Aziz,[2] and Oliver Kühn[1]
[1]Institut für Physik, Universität Rostock, Albert-Einstein-Str. 23-24, 18059 Rostock, Germany
[2]Chemistry Department, Faculty of Science, King Abdulaziz University, 21589 Jeddah, Saudi Arabia
(Received 27 July 2016; revised manuscript received 16 September 2016; published 10 January 2017)

Recent advances in attosecond physics provide access to the correlated motion of valence and core electrons on their intrinsic timescales. For valence excitations, processes related to the electron spin are usually driven by nuclear motion. For core-excited states, where the core hole has a nonzero angular momentum, spin-orbit coupling is strong enough to drive spin flips on a much shorter time scale. Here, unprecedented short spin crossover is demonstrated for L-edge ($2p \rightarrow 3d$) excited states of a prototypical Fe(II) complex. It occurs on a time scale, which is faster than the core-hole lifetime of about 4 fs and can be manipulated by the excitation conditions. A detailed analysis of such phenomena will help to gain a fundamental understanding of spin-crossover processes and establish the basis for their control by light.

DOI: 10.1103/PhysRevLett.118.023001

The rapid development of gas-phase and surface high-harmonic generation techniques paves the way to study ultrafast processes occurring in the soft-x-ray domain [1–3] and on ultrashort time scales approaching few tens of attoseconds [4]. The novel light sources provide a tool to measure, trigger, and control ultrafast electronic processes in atoms, molecules, and nanoparticles for both valence and more tightly bound core electrons via preparation of intricate superpositions of quantum states [5–7]. Attosecond spectroscopy has a huge potential to study atomic and molecular responses to incident light [8,9], thus giving access to, for example, electron correlation manifesting itself in the entanglement of bound and photo electrons (shakeups), Auger and interatomic Coulomb decay, as well as to the coupling of electrons in plasmonic systems [5–7,10]. Further, progress has been seen for the understanding of the dynamics of charge (hole) migration in molecules driven solely by electron correlation [10–15]. Microscopic understanding of such ultrafast transfer phenomena is essential, e.g., to approach the fundamental limits of the transmission speed of signals relevant for molecular electronics.

Devices based on spin-polarized currents are a prospective extension of conventional electronics [16,17]. Recently, spin-crossover dynamics attracted much attention, e.g., in the context of high-density magnetic data storage devices [18,19]. Popular materials are based on Fe(II) organometallic complexes. Because of their partially filled $3d$ shell, they feature low- as well as high-spin electronic states. Upon valence excitation, these systems exhibit an ultrafast spin crossover, occurring on time scales of the order of 100 fs [20]. The spin-orbit couplings (SOC) between valence-excited states, however, are small, and spin crossover is essentially driven by nuclear motion since it requires the nuclear wavepacket to pass through a region of near degeneracy of two states of different multiplicity. Thus, the time scale is determined by the related vibrational periods (see also Ref. [21]). In passing, we note that this is also a typical time scale for spin transfer between magnetic centers in polynuclear metal complexes [22].

For core-excited electronic states of transition metal complexes, however, the magnitude of SOC increases dramatically. Therefore, one expects the spin dynamics to change from a nuclear to an electronically driven process. In this Letter, it will be demonstrated for the first time that electronically driven spin crossover after core-hole excitation in transition metals indeed takes place on a few femtoseconds time scale. Further, the design of a possible experimental setup to study such ultrafast spin dynamics is discussed.

The ultrafast spin-flip process is investigated using the time-dependent restricted-active-space configuration-interaction (TD RASCI) method, which is similar in spirit to the techniques proposed in Refs. [22–24], but expands on the interplay between electronic correlation and spin dynamics. Here, the electronic wave function within clamped nuclei approximation is represented in the basis of Configuration State Functions (CSFs), $\Phi_j^{(S,M_S)}$, with the total spin S and its projection M_S:

$$|\Psi(t)\rangle = \sum_j c_j^{(S,M_S)}(t) \left| \Phi_j^{(S,M_S)} \right\rangle. \tag{1}$$

The CSFs are obtained using a fixed molecular orbital basis, optimized at the restricted active space self-consistent field [25] level prior to propagation. The Hamiltonian in the CSF basis reads

$$\begin{aligned} \mathbf{H}(t) &= \mathbf{H}_{\mathrm{CI}} + \mathbf{V}_{\mathrm{SOC}} + \mathbf{U}_{\mathrm{ext}}(t) \\ &= \begin{pmatrix} \mathbf{H}_h & 0 \\ 0 & \mathbf{H}_l \end{pmatrix} + \begin{pmatrix} \mathbf{V}_{hh} & \mathbf{V}_{hl} \\ \mathbf{V}_{lh} & \mathbf{V}_{ll} \end{pmatrix} + \begin{pmatrix} \mathbf{U}_h(t) & 0 \\ 0 & \mathbf{U}_l(t) \end{pmatrix}, \end{aligned} \tag{2}$$

where we separated blocks of low (l) and high (h) spin states. In Eq. (2), $\mathbf{H}_{\mathrm{CI}}$ is the configuration interaction (CI) Hamiltonian containing the effect of electron correlation. The eigenstates of the spin-free Hamiltonian $\mathbf{H}_{\mathrm{CI}}$ will be called spin free (SF) states. SOC is contained in $\mathbf{V}_{\mathrm{SOC}}$, whose matrix elements are calculated within a perturbative LS-coupling scheme, based on atomic mean-field integrals, which is an effective one-electron approximation to the Breit-Pauli equation [26]. This method has demonstrated good performance for L-edge spectra of transition metal compounds [27–29]. It provides an intuitive interpretation in terms of pure spin states with well-defined S and M_S quantum numbers. The eigenstates of $\mathbf{H}_{\mathrm{CI}} + \mathbf{V}_{\mathrm{SOC}}$ are called SOC states. The interaction with the time-dependent electric field, $\mathbf{U}_i = -\vec{\mathbf{d}}_{ii} \cdot \vec{E}(t)$, is taken in a semiclassical dipole approximation, with the transition dipole matrices $\vec{\mathbf{d}}_{ii}$ and the field vector $\vec{E}(t)$ having a carrier frequency Ω and a Gaussian envelope, i.e., $E(t) = E_0 \cos(\Omega t) \exp[-t^2/(2\sigma^2)]$. The resulting time-dependent Schrödinger equation has been solved with the Runge-Kutta-Fehlberg method using adaptive step size control. The time steps did range from 2.5 as, when the external field was small or absent, down to 0.09 as when the interaction with the pulse was substantial.

In the following, the outlined approach is applied to the spin-flip dynamics in $[\mathrm{Fe}(\mathrm{H_2O})_6]^{2+}$, whose x-ray absorption and resonant inelastic x-ray scattering characteristics have been studied in Refs. [28,30,31]. The active space used in TD RASCI calculations contains 12 electrons distributed over the three $2p$ (one hole allowed) and five $3d$ (full CI) orbitals to describe the core-excited electronic states corresponding to the dipole allowed $2p \rightarrow 3d$ transitions [28,30–32]. This active space includes up to $4h4p$ configurations and results in 35 quintet ($S = 2$) and 195 triplet ($S = 1$) electronic states, directly interacting via SOC, according to the $\Delta S = 0, \pm 1$ selection rule. Accounting for the different M_S components, the total amount of SF and SOC states is 760, where 160 are valence and 600 core ones. Notice that both the account for $4h4p$ excitations and SOC are essential to recover the dynamics of the highly correlated core-excited states. Evaluation of the matrix elements of $\mathbf{H}_i$, $\mathbf{V}_{ij}$, and $\vec{\mathbf{d}}_{ii}$ in the CSF basis has been performed with a locally modified MOLCAS 8.0 [33] quantum chemistry package, applying the atomic-natural-orbital relativistic core-correlation triple-ζ valence plus polarization (ANO RCC TZVP) basis set [34,35] for all atoms.

In Fig. (1a), the L-edge absorption spectrum of $[\mathrm{Fe}(\mathrm{H_2O})_6]^{2+}$ is shown for further reference. It has a shape characteristic for transition metals, featuring the L_3 ($J = 3/2$) and L_2 ($J = 1/2$) bands split due to the SOC. This splitting is 12.7 eV (SOC constant is 8.5 eV), which corresponds to a time scale of about 0.33 fs. Panel (b) of Fig. 1 illustrates the degree of spin mixing for the SOC states. It can be seen that the valence-excited states are mostly pure quintets or triplets. In contrast, the core-excited states are dominantly spin mixtures.

The dynamics discussed below are driven solely by electronic SOC, while nuclei are fixed at the ground state equilibrium positions. To justify the use of the clamped nuclei approximation, we assume that the system is excited far from conical intersections and that the considered time interval is shorter than the relevant vibrational periods. For $[\mathrm{Fe}(\mathrm{H_2O})_6]^{2+}$, the Fe–O stretching and O–Fe–O deformation modes possibly influencing the $2p \rightarrow 3d$ core-excited electronic states have periods above 100 fs.

In the following, we will discuss two different cases, illustrating the dynamics of ultrafast spin crossover. In case I, $\vec{E}(t) = 0$, and it is assumed that a particular SF state has been prepared. This somewhat artificial initial condition, which would, in general, require complex-shaped circularly polarized pulses with sub-200 as duration, will serve as a reference, which highlights the spin dynamics driven solely by SOC. In case II, the system is initially in the ground state, with the M_S components of the lowest closely lying electronic states being populated according to the Boltzmann distribution at 300 K. The core hole is created and thus, spin dynamics are driven by an ultrashort x-ray pulse, $\vec{E}(t)$, which is linearly polarized along the shortest of the Fe–O bonds. The spectral overlaps of the different pulses with the SOC states are shown in Fig. (1b) as numbered ranges.

Case I.—We have selected two quintet SF states, i.e., numbers 7 and 111, denoted as $\mathrm{SF_{val}}$ and $\mathrm{SF_{core}}$, respectively, as initial states for investigating the SOC-driven spin dynamics; for the contributions of $\mathrm{SF_{val}}$ and $\mathrm{SF_{core}}$ to the SOC states, see Fig. (1b). These two states have been chosen as typical representatives of valence- and core-excited levels, with other states showing similar dynamics. $\mathrm{SF_{val}}$ is a superposition of valence-excited SOC states and it features a rather weak SOC, such that there are little dynamics within the considered time window of 15 fs (see Supplemental Material [36]). Hence, it will not be discussed further. In contrast, $\mathrm{SF_{core}}$, which corresponds to $M_S = +2$ (four spin-up electrons) has contributions of SOC states from essentially the whole core-hole excited L_3 and L_2 bands [cf. blue bars in Fig. (1b)].

Panels (c) and (d) of Fig. 1 show snapshots of the time evolution of the spin-density difference, $\rho_\uparrow - \rho_\downarrow$ and the total populations of all quintet and triplet states, respectively. A more detailed analysis in terms of the different M_S components is given in the Supplemental Material [36]. As a consequence of SOC, the population spreads over both quintet and triplet states such that the total triplet population becomes even larger than the corresponding quintet one within about 1 fs [Fig. (1d)]. The population transfer occurs stepwise according to the $\Delta M_S = 0, \pm 1$ selection rule within and between both spin manifolds. The main contribution to the fast drop of the quintet population during the first few fs is due to the $(S = 2, M_S = +2) \rightarrow (S = 1, M_S = +1)$ transitions. Quintets with $M_S = -1$ and -2 start

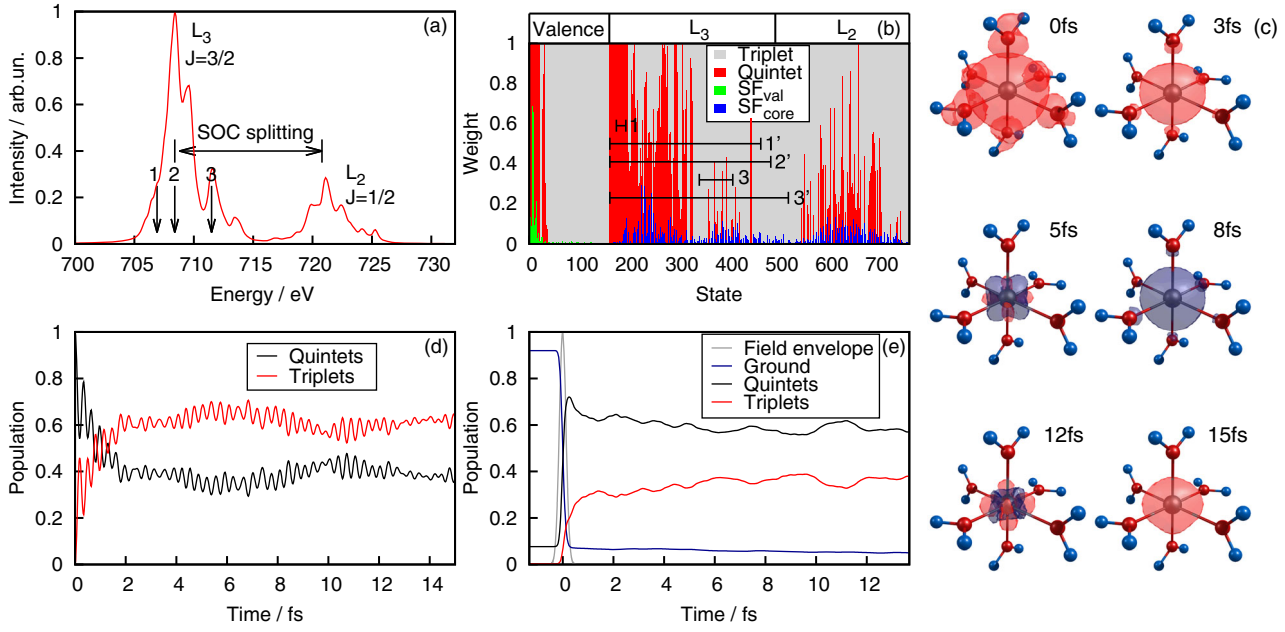

FIG. 1. (a) X-ray absorption spectrum of $[Fe(H_2O)_6]^{2+}$; arrows denote the excitation energies considered in case II, see text. (b) Collective contributions of the quintet (red bars) SF states to the stationary SOC eigenstates ($\sum_{j,M_S}|c_j^{(S=2,M_S)}|^2$, see Eq. (1); the grey areas correspond to the triplet SF states ($\sum_{j,M_S}|c_j^{(S=1,M_S)}|^2$), which together with quintet ones, sum up to unity. The particular contributions of valence SF states (SF_{val}, green bars) and core SF states (SF_{core}, blue bars) to the different SOC states are also shown. Numbered ranges reflect the bandwidths of 0.5 eV (1 and 3) and 5.0 eV (1', 2', and 3') pulses, with carrier frequencies denoted in panel (a), in terms of the involved SOC states. (c) Evolution of spin-density difference, $\rho_\uparrow - \rho_\downarrow$ (red—positive, blue—negative, contour value 0.001), obtained in case I for an initial state, which corresponds to the SF_{core}, with $M_S = +2$. (d) Evolution of the total population of the quintet and triplet electronic states after instantaneous excitation to the SF_{core} state (case I). (e) Evolution of the total population of the quintet and triplet electronic states after explicit field excitation (case II), with the pulse centered at $\hbar\Omega = 708.4$ eV, having a bandwidth of $\hbar/\sigma = 5.0$ eV and $E_0 = 2.5\, E_h e^{-1}\text{bohr}^{-1}$. The envelope of the excitation pulse is shown in grey. The population of M_S components of the ground state is shown by the blue line.

to be populated only after about 1 fs. Because of this quintet-triplet population transfer, $\rho_\uparrow$ notably decreases during the first 3 fs [Fig. (1c)]. After about 4 fs, the system almost equilibrates, i.e., the 760 electronic states act like an "electronic bath." The corresponding populations of M_S components oscillate around their mean value (see Supplemental Material [36]). The spin density changes relatively slowly from the dominating $\rho_\uparrow$ to the dominating $\rho_\downarrow$ and back due to the partial revivals of quintet's positive and negative spin projections. The fast modulation in Fig. (1d) with a period of ≈0.32 fs can be assigned to the SOC splitting between the L_2 and L_3 bands. It is roughly the same for all interacting states and is an intrinsic property of the $2p$ core hole. To sum up, core-excited states demonstrate unprecedentedly fast purely electronic spin-flip dynamics, which is two orders of magnitude faster than that driven by nuclear motion in conventional spin crossover [20].

Case II.—Next, we consider the more realistic situation of an excitation with Gaussian-shaped, linearly polarized pulses having temporal duration of $\sigma = 0.8$ and 8.3 fs (bandwidths $\hbar/\sigma = 5.0$ and 0.5 eV), respectively. The spin dynamics upon excitation, with a light pulse with bandwidth of 5.0 eV centred at 708.4 eV [labeled 2 in Figs. (1a) and (1b)], is shown in Fig. (1e). For this excitation condition, the ultrafast spin-flip process also occurs as in the case I, but the population of all triplet states stays below 40% within the time period of 15 fs.

Note that the field strengths (see Fig. 2), despite their large magnitudes, at soft-x-ray wavelengths correspond to the weak-field regime with Keldysh parameter $\gamma > 7$. Moreover, the transition dipoles are quite small and the Rabi energy with respect to the strongest transition is $d_{\max}E_0 = 2.7$ eV and 1.6 eV for the spectrally broad and the narrow pulse, respectively. In fact, E_0 has been chosen merely to have an appreciable depletion of the ground state for illustration purposes. Indeed, the dynamics triggered by much weaker pulses coincide qualitatively with the present one, see Supplemental Material [36].

The actual degree of quintet-triplet spin mixing is rather sensitive to the excitation conditions. This is shown in Fig. 2 where the spin dynamics are given for two different excitation frequencies, 706.9 and 711.5 eV, and two bandwidths, 0.5 and 5.0 eV. Here, the excitation frequencies correspond to spectral regions with small and notable SOC mixing [cf. the arrows in Fig. (1a) and the numbered ranges in Fig. (1b)]. The pulse amplitude has been chosen

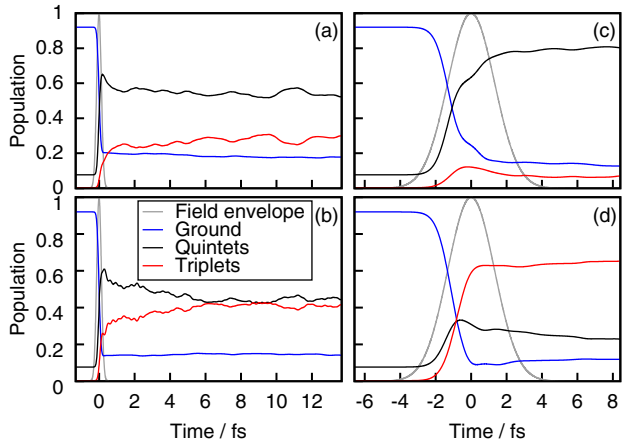

FIG. 2. Spin dynamics initiated by the explicit field excitation with different carrier frequencies and bandwidths corresponding to: (a) 706.9 eV and 5.0 eV, (b) 711.5 eV and 5.0 eV, (c) 706.9 eV and 0.5 eV, (d) 711.5 eV and 0.5 eV, respectively [for the spectral overlap with the SOC states, cf. Fig. (1b)]. The field amplitude is $E_0 = 2.5E_h e^{-1}\text{bohr}^{-1}$ for panels (a) and (b), and $E_0 = 1.5E_h e^{-1}\ \text{bohr}^{-1}$ for (c) and (d).

such as to yield a similar depletion of the ground state of about 80% (blue curves, Fig. 2). The spectral selectivity with respect to the spin mixing is fairly pronounced: a slight modification of the excitation frequency from 706.9 eV to 711.5 eV changes the quintet/triplet ratio at 15 fs from 0.4 to 11.3 [see Figs. (2c) and (2d)].

As compared with case I, most notable is the absence of the rapid oscillations. This is due to the fact that the temporal width of the pulse is longer than the 0.3 fs oscillation period dictated by SOC, i.e., the effect is smeared out. Further, there are more slowly oscillating components in Fig. (1e) than in case I. This can be traced to the fact that the initial state before excitation is an incoherent thermal mixture of different M_S components. Excitation with linearly polarized light (in the absence of a magnetic field) leads to equal populations of $\pm M_S$ components, see Supplemental Material [36]. Hence, the pattern of $\Delta M_S = 0, \pm 1$ transitions, which are possible upon excitation, changes. Comparing Figs. (2a) and (2b) with Fig. (1e), one notices similar oscillations, but decreasing the bandwidth of the pulses [panels (c) and (d)] washes out the oscillations almost completely.

The striking dependence of spin ratios on the pulse parameters being established within a few femtoseconds calls for an experimental verification. The most direct way to access the spin dynamics would be time-resolved nonlinear x-ray spectroscopy, e.g., stimulated resonant inelastic x-ray scattering (SRIXS) [37–39]. With this technique, one projects the mixed-spin core states onto the manifold of pure-spin valence states, which are usually energetically well separated in transition metal complexes, see e.g., discussion in Refs. [31,40]. Thus, the relative SRIXS intensities in the respective energy ranges (0–1.5 eV for quintets and 1.5–8.2 eV for triplets in the case of $[Fe(H_2O)_6]^{2+}$ system), resolved in time, would allow one to judge on the evolution of the contribution of pure spin states to a mixed one.

Summarizing, we have studied the spin-flip dynamics, which are driven solely by SOC on a time scale where nuclear motion can be neglected. Such dynamics should be typical for states having core holes with a nonzero orbital momentum. This process can be considered as an elementary step of the conventional nuclear dynamics driven spin crossover [18], analogously to charge migration [13] being an elementary step of electron-nuclear dynamics leading to charge transfer [41]. In both cases, electronic wave packet dynamics are ultimately coupled to nuclear motions, eventually leading to charge or spin localization. Using the example of a prototypical third period transition metal complex, it has been demonstrated that soft-x–ray light can trigger spin dynamics, which are faster than the lifetime of the $2p$ core hole ($\approx$4 fs and $\approx$10 fs for Fe L_2 and L_3, respectively) [42]. Interestingly, the actual spin mixture can be controlled to quite some extent with modest effort, i.e., by small changes of pulse duration and carrier frequency. Although the reported ultrafast spin-flip process is of predominant intra-atomic character, we expect the dynamics to be influenced by the chemical environment (ligands), especially in cases where covalent ligand-metal interactions substantially change the electronic structure.

Given the recent progress in high-harmonic generation [1–4] and free-electron lasers [8] and the upcoming establishment of time-resolved techniques, such as SRIXS [37–39], the experimental verification of the ultrafast purely electronically driven spin-flip process and its use for manipulating spin dynamics appears to be within reach.

We acknowledge financial support by the Deanship of Scientific Research (DSR), King Abdulaziz University, Jeddah, (Grant No. D-003-435).

*sergey.bokarev@uni-rostock.de

[1] B. Dromey, M. Zepf, A. Gopal, K. Lancaster, M. S. Wei, K. Krushelnick, M. Tatarakis, N. Vakakis, S. Moustaizis, R. Kodama, M. Tampo, C. Stoeckl, R. Clarke, H. Habara, D. Neely, S. Karsch, and P. Norreys, Nat. Phys. **2**, 456 (2006).
[2] P. Zhang and A. G. R. Thomas, Appl. Phys. Lett. **106**, 131102 (2015).
[3] D. Popmintchev *et al.*, Science **350**, 1225 (2015).
[4] S. M. Teichmann, F. Silva, S. L. Cousin, M. Hemmer, and J. Biegert, Nat. Commun. **7**, 11493 (2016).
[5] M. F. Kling and M. J. J. Vrakking, Annu. Rev. Phys. Chem. **59**, 463 (2008).
[6] F. Krausz and M. Ivanov, Rev. Mod. Phys. **81**, 163 (2009).
[7] F. Lépine, G. Sansone, and M. J. Vrakking, Chem. Phys. Lett. **578**, 1 (2013).
[8] A. Picón *et al.*, Nat. Commun. **7**, 11652 (2016).
[9] D. Healion, Y. Zhang, J. D. Biggs, N. Govind, and S. Mukamel, J. Phys. Chem. Lett. **3**, 2326 (2012).

[10] G. Sansone, T. Pfeifer, K. Simeonidis, and A. I. Kuleff, ChemPhysChem **13**, 661 (2012).
[11] H. Hennig, J. Breidbach, and L. S. Cederbaum, J. Phys. Chem. A **109**, 409 (2005).
[12] F. Remacle and R. D. Levine, Proc. Natl. Acad. Sci. U.S.A. **103**, 6793 (2006).
[13] A. I. Kuleff and L. S. Cederbaum, J. Phys. B **47**, 124002 (2014).
[14] F. Calegari, D. Ayuso, A. Trabattoni, L. Belshaw, S. D. Camillis, S. Anumula, F. Frassetto, L. Poletto, A. Palacios, P. Decleva, J. B. Greenwood, F. Martín, and M. Nisoli, Science **346**, 336 (2014).
[15] P. M. Kraus, B. Mignolet, D. Baykusheva, A. Rupenyan, L. Horný, E. F. Penka, G. Grassi, O. I. Tolstikhin, J. Schneider, F. Jensen, L. B. Madsen, A. D. Bandrauk, F. Remacle, and H. J. Wörner, Science **350**, 790 (2015).
[16] T. Dietl, D. D. Awschalom, M. Kaminska, H. Ohno, Spintronics in *Semiconductors and Semimetals* (Academic Press, Amsterdam, 2008), Vol. 82.
[17] S. Bader and S. Parkin, Annu. Rev. Condens. Matter Phys. **1**, 71 (2010).
[18] A. Cannizzo, C. Milne, C. Consani, W. Gawelda, Ch. Bressler, F. van Mourik, and M. Chergui, Coord. Chem. Rev. **254**, 2677 (2010).
[19] M. A. Halcrow, in *Spin-Crossover Materials* (John Wiley & Sons, New York, 2013) pp. 147–169.
[20] G. Auböck and M. Chergui, Nat. Chem. **7**, 629 (2015).
[21] M. Bargheer, R. B. Gerber, M. V. Korolkov, O. Kühn, J. Manz, M. Schröder, and N. Schwentner, Phys. Chem. Chem. Phys. **4**, 5554 (2002).
[22] W. Jin, F. Rupp, K. Chevalier, M. M. N. Wolf, M. C. Rojas, G. Lefkidis, H.-J. Krüger, R. Diller, and W. Hübner, Phys. Rev. Lett. **109**, 267209 (2012).
[23] J. C. Tremblay, S. Klinkusch, T. Klamroth, and P. Saalfrank, J. Chem. Phys. **134**, 044311 (2011).
[24] T. Kato, T. Oyamada, H. Kono, and S. Koseki, Prog. Theor. Phys. Suppl. **196**, 16 (2012).
[25] P.-Å. Malmqvist, A. Rendell, and B. O. Roos, J. Phys. Chem. **94**, 5477 (1990).
[26] B. A. Heß, C. M. Marian, U. Wahlgren, and O. Gropen, Chem. Phys. Lett. **251**, 365 (1996).
[27] I. Josefsson, K. Kunnus, S. Schreck, A. Föhlisch, F. de Groot, P. Wernet, and M. Odelius, J. Phys. Chem. Lett. **3**, 3565 (2012).
[28] S. I. Bokarev, M. Dantz, E. Suljoti, O. Kühn, and E. F. Aziz, Phys. Rev. Lett. **111**, 083002 (2013).
[29] C. J. Milne, T. J. Penfold, and M. Chergui, Coord. Chem. Rev. **277–278**, 44 (2014).
[30] K. Atak, S. I. Bokarev, M. Gotz, R. Golnak, K. M. Lange, N. Engel, M. Dantz, E. Suljoti, O. Kühn, and E. F. Aziz, J. Phys. Chem. B **117**, 12613 (2013).
[31] R. Golnak, S. I. Bokarev, R. Seidel, J. Xiao, G. Grell, K. Atak, I. Unger, S. Thürmer, S. G. Aziz, O. Kühn, B. Winter, and E. F. Aziz, Sci. Rep. **6**, 24659 (2016).
[32] G. Grell, S. I. Bokarev, B. Winter, R. Seidel, E. F. Aziz, S. G. Aziz, and O. Kühn, J. Chem. Phys. **143**, 074104 (2015).
[33] F. Aquilante *et al.*, J. Comput. Chem. **37**, 506 (2016).
[34] B. O. Roos, R. Lindh, P.-Å. Malmqvist, V. Veryazov, and P.-O. Widmark, J. Phys. Chem. A **108**, 2851 (2004).
[35] B. O. Roos, R. Lindh, P.-Å. Malmqvist, V. Veryazov, and P.-O. Widmark, J. Phys. Chem. A **109**, 6575 (2005).
[36] See Supplemental Material at http://link.aps.org/supplemental/10.1103/PhysRevLett.118.023001 for dynamics of the different M_S components for cases I and II and comparison of dynamics for different field strengths.
[37] S. Mukamel, D. Healion, Y. Zhang, and J. D. Biggs, Annu. Rev. Phys. Chem. **64**, 101 (2013).
[38] D. J. Haxton and C. W. McCurdy, Phys. Rev. A **90**, 053426 (2014).
[39] Y. Zhang, W. Hua, K. Bennett, and S. Mukamel, Top. Curr. Chem. **368**, 273 (2015).
[40] S. I. Bokarev, M. Khan, M. K. Abdel-Latif, J. Xiao, R. Hilal, S. G. Aziz, E. F. Aziz, and O. Kühn, J. Phys. Chem. C **119**, 19192 (2015).
[41] V. May and O. Kühn, *Charge and Energy Transfer Dynamics in Molecular Systems*, 3rd ed. (Wiley-VCH, Weinheim, 2011).
[42] M. Ohno, J. Electron Spectrosc. Relat. Phenom. **171**, 1 (2009).